Journal of Oceanology and Limnology
Vol. 39 No. 1, P. 350-361, 2021
https://doi.org/10.1007/s00343-020-9302-7

Comparative transcriptome analysis of abalone *Haliotis discus hannai* with green and gray egg colors*

Yanwei FENG[1, **, #], Bo YUAN[2, 3, 4, #], Xu JIANG[5], Xiangquan LIU[2, **], Zan LI[1], Guohua SUN[1], Xiaohui XU[1]

[1] *School of Agriculture, Ludong University, Yantai 264025, China*

[2] *Shandong Provincial Key Laboratory of Restoration for Marine Ecology, Shandong Marine Resource and Environment Research Institute, Yantai 264006, China*

[3] *National Demonstration Center for Experimental Fisheries Science Education, Shanghai Ocean University, Shanghai 201306, China*

[4] *Shanghai Engineering Research Center of Aquaculture, Shanghai Ocean University, Shanghai 201306, China*

[5] *Shandong Rice Research Institute, Shandong Academy of Agricultural Sciences, Jinan 250100, China*

Received Dec. 6, 2019; accepted in principle Jan. 26, 2020; accepted for publication Apr. 1, 2020

Abstract *Haliotis discus hannai* is an important marine economic species in China. Its egg color was found to be associated with economic traits, which provides a new idea for breeding. However, the molecular mechanism of the egg-color formation has not been reported. Thus, the pigment composition and comparative transcriptome analyses of *H. discus hannai* with green and gray egg color were conducted using high-performance liquid chromatography (HPLC) and RNA-Seq methods. Results show that individuals with green and gray eggs both possess the fucoxanthin. Lutein existed in gray-egged individuals, but not in green-egged individuals. In transcriptome analysis, 272 310 unigenes were received from 461 162 transcripts with a mean length of 985 bp and N50 of 1 524 bp, respectively. A total of 185 unigenes were identified as differentially expressed genes (DEGs). The DEGs involved in "flavin-containing compound metabolic process", "melanosome", "glutathione metabolism", and "cytochrome b6f complex" were likely related to the formation of the egg color. Our results provide foundational information for the functional analysis of egg-color related genes and are beneficial to the selective breeding of *H. discus hannai*.

Keyword: *Haliotis discus hannai*; egg color; high-performance liquid chromatography; transcriptome; differentially expressed genes

1 INTRODUCTION

Haliotis discus hannai, which belongs to Mollusca, Gastropoda, is regarded as the most important cultivated abalone in China, Japan, and South Korea. It is known for its high nutritional value and high market value (Gordon and Cook, 2004). However, with the increasing density of culture and the deterioration of farming environment, many problems appeared, such as high mortality, slow growth, and poor resistance. It is urgent to develop new cultured strains.

Many efforts have focused on developing new strains by selective breeding (Symonds et al., 2012) and heterosis (You et al., 2009), but these are far from enough. Egg color may be closely related to specific economic traits. Hulet et al. (1978) reported that hatchability of brown and olive eggs was higher than that of blue and white eggs in pheasant. Cooley (1971) found the green eggs of *Dinptomus oregonensis* had a lower diapause rate than red eggs. Our team found that the growth index and immune enzyme activity of *H. discus hannai* with green egg-color were higher than other egg-colors' (Zhao et al., 2016), which provides a new idea for the breeding of abalone. As

* Supported by the Seed Improvement Project of Shandong Province of China (No. 2017LZGC009) and the Major Scientific and Technological Innovation Project of Shandong Provincial Key Research and Development Program (No. 2019JZZY020706)
** Corresponding authors: fywzxm1228@163.com; lxq6808@163.com
# Yanwei FENG and Bo YUAN contributed equally to this work and should be regarded as co-first authors.

the conventional breeding are time-consuming and labor-intensive, marker-assisted selection (MAS) was used to accelerate the progress of breeding greatly. However, the related markers and genes of egg-color were not reported in *H. discus hannai*.

The information provided by transcriptome analysis can reveal gene expression profiles and speculate unknown gene functions (Liu et al., 2015). RNA-Seq is a more efficient, rapid, and sensitive method for deeply studying and analyzing the transcriptome of organisms (Metzker, 2010). Now, RNA-Seq has been applied in many aquatic animals, such as Oujiang carp (*Cyprinus carpio* var. *color*) (Wang et al., 2014), small abalone (*Haliotis diversicolor*) (Zhang et al., 2019), Whitefish (*Coregonus clupeaformis* spp.) (Jeukens et al., 2010), California red abalone (*Haliotis rufescens*) (Valenzuela-Miranda et al., 2015), Japanese scallop (*Patinopecten yessoensis*) (Ding et al., 2015), European abalone (*Haliotis tuberculata*) (Harney et al., 2016), and Pacific white shrimp (*Litopenaeus vannamei*) (Guo et al., 2013). For *H. discus hannai*, the transcriptome analyses were mainly concentrated in reproduction (Kim et al., 2017), growth (Choi et al., 2015), and immunity (Nam et al., 2016; Shen et al., 2019), its egg color trait was not involved.

In this study, we analyzed the pigments existed in gonad of *H. discus hannai* by high-performance liquid chromatography (HPLC) and conducted a comparative transcriptome analysis between gray- and green-egged individuals in order to identify some differentially expressed genes and pathways that may determine egg-color formation. Our results will provide foundational information for further studying the molecular mechanism of egg coloring in *H. discus hannai*.

2 MATERIAL AND METHOD

2.1 Sample collection

The individuals of *H. discus hannai* were collected from Xunshan Breeding Base in Weihai, Shandong Province, China, in December 2017. Five gray- and five green-egged female individuals were chosen. The gonads and eggs are shown in Fig.1. All individuals under the same condition and were cultured under a standardized feeding regimen. The gonads of all samples were dissected and then stored at -80 °C.

2.2 HPLC analysis

Five green- and five gray-egged female individuals were used to analyze the differences of pigments in gonads by HPLC. Fucoxanthin, astaxanthin, canthaxanthin, lutein, zeaxanthin and β-carotene were used as standards. The pigments were extracted with acetone, leached with petroleum ether, separated by pure water, and purified by LC-NH2. The analysis was carried out with ZORBAXEclipse SB-C18 column (Agilent, California, USA, 250 mm×4.6 mm, 5 μm) and determined at 450 nm. The mobile phase consisted of methanol:water (98:2). The types of pigments were determined by comparing the chromatogram of samples with standards.

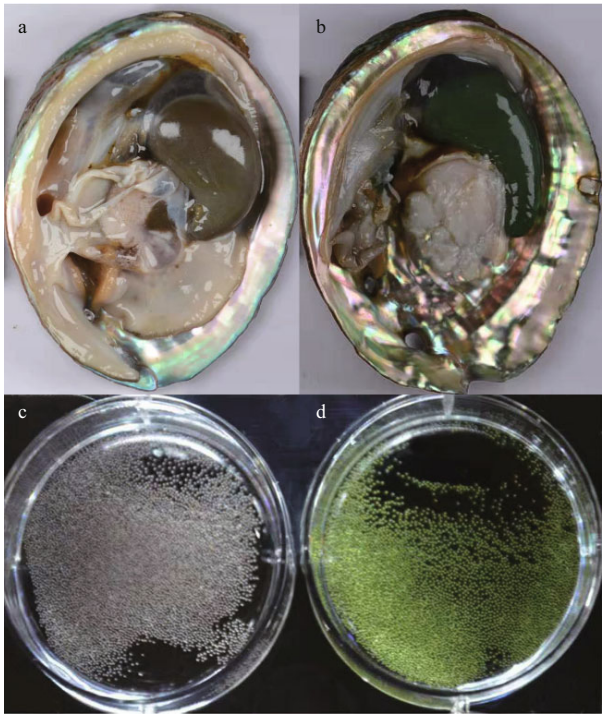

Fig.1 The gonads and eggs of *Haliotis discus hannai*

a. the gonad tissue of gray-egged individual; b. the gonad tissue of green-egged individual; c. the gray eggs; d. the green eggs.

2.3 Total RNA isolation, library construction and sequencing

Total RNA was extracted from three gray- (H1, H2, and H3) and three green-egged (L1, L2, and L3) female individuals using the TRIzol™ Reagent (Invitrogen, California, USA). RNA quality was detected by NanoDrop One^c spectrophotometer (Thermo, Massachusetts, USA), agarose gel electrophoresis, and Agilent 2100 (Agilent, California, USA). A total amount of 1.5-μg RNA per sample was used to construct cDNA libraries using NEBNext® Ultra™ RNA Library Prep Kit for Illumina® (NEB, Massachusetts, USA). Briefly, total RNA was performed to purify mRNA by poly-T oligo-attached magnetic beads. First cDNA strand was obtained

using random hexamer primer and M-MuLV Reverse Transcriptase (RNase H), which was followed by the synthesis of second strand. The purified double-stranded cDNA was end-repaired and added with "A" tail and adapters. AMPure XP beads were used for fragment size selection. The 250–300-bp fragments were amplified and purified to obtain the final library, followed by sequencing on Illumina Hiseq platform.

2.4 Transcripts assembly and annotation

Transcriptome assembly was performed using the program Trinity (Li and Durbin, 2009) with min_kmer_cov set to 2 and other parameters set default, and the longest transcript under each gene was regarded as unigene (Altschul et al., 1990). All unigenes function was annotated against NCBI non-redundant protein sequences (NR) (Deng et al., 2006), Gene Ontology (GO) (Ashburner et al., 2000), Swiss protein sequences (Swiss-Prot) (Apweiler et al., 2004), euKaryotic Ortholog Groups (KOG) (Huerta-Cepas et al., 2015), Kyoto Encyclopedia of Genes and Genomes (KEGG) (Kanehisa et al., 2004), and Protein family (Pfam) (Finn et al., 2013) databases.

2.5 Analysis of gene expression levels

Gene expression levels of the samples were estimated using RSEM (Li and Dewey, 2011). Clean reads were matched back to the assembled transcriptome. Readcount of each unigene was acquired from the matching results and then normalized to FPKM (Trapnell et al., 2010).

The DESeq R package (1.10.1) was used to conduct differential expression analysis of two groups. DESeq provides statistical routines for determining differential expression genes and the false discovery rate was limited by adjusting the resulting *P*-values. Genes with an adjusted $P<0.05$ and fold-change ≥ 2 were identified as significantly differential expression.

2.6 GO/KEGG enrichment analysis of DEGs

GO analysis of the differentially expressed genes (DEGs) was implemented by the GOseq R packages (Young et al., 2010). The calculated *P*-value goes through Bonferroni Correction, taking <0.05 as the threshold. The statistical enrichment of DEGs in KEGG pathways was tested using KOBAS (Mao et al., 2005) software.

2.7 Quantitative RT-PCR verification

To validate the reliability of our DEGs data, quantitative RT-PCR analysis was conducted on 9 randomly selected genes. The same batch of RNA samples as sequenced was used, and the cDNA was synthesized using the PrimeScript™RT reagent Kit with gDNA Eraser (TaKaRa, Dalian, China). The used primers were designed using Primer Premier 5.0 software and are listed in Table 1. Quantitative RT-PCR was carried out using TB Green™ Premix Ex Taq™ (TaKaRa, Dalian, China) in the LightCycler® 480 II Real Time instrument (Roche, Rotkreuz, Switzerland). The cycling conditions were 95 °C for 2 min; followed by 40 cycles of 95 °C for 15 s, 60 °C for 15 s and 72 °C for 1min; melt curve detection of 60 °C for 5 s to 95 °C increment 0.11 °C. The relative mRNA expression levels were calculated by normalizing to the reference genes (β-actin) (Wang, 2015). Three replicates were performed independently for each gene. Relative gene expression levels were calculated with the $2^{-\Delta\Delta Ct}$ comparative cycle threshold (C_t) method (Livak and Schmittgen, 2001).

Table 1 Sequences of primers used in qRT-PCR analysis

Gene name	Primer sequence (5′→3′)	Length of product (bp)
SoCYT	F AGACGTTGTTGCTATGCTGAACTG	164
	R TTCTCCTACTGGGGCTTGTCGT	
GLT1	F GATGTACCTCCTGCGGAAGTATG	192
	R GAGAAGCGACTGTGGATAAGGG	
PNKD	F TTTCTGCACTGGCTCTGGGTC	257
	R GAGGCTGTTTCTTCAGGATTGG	
Protein melan-A	F TGCTCTGATGCTTTCTTCGTCTAC	192
	R ACATTGCGTCACAGTCGTTCC	
PPIP5K2	F AAGGTTCTATCAAGGGCTCGG	185
	R CCAGTCCCATTCTGGCATGT	
CD109	F ATTATTGGAGGAGACGCAGGC	277
	R TGCTGGGGTCAAACATCTCG	
A2M	F ACTGCTCTTCTACTGGCTTCTCAAC	146
	R CATCAATGGCAAGAACGCAC	
Alpha-macroglobulin	F GTGTTGATGTCCCAATGTCTGTC	149
	R GGCAGTTGATGGATCATACAGG	
CPAMD8	F TTGGTAGAACGCCACTGCCT	92
	R GAAGGAATGGTCAGGTTGCTAAG	
β-actin	F CACGGGTATTGTTCTGGACTCTG	
	R ATGAGGTAGTCTGTGAGGTCACGTC	

3 RESULT

3.1 HPLC analysis

The chromatogram of mixed standard solution is

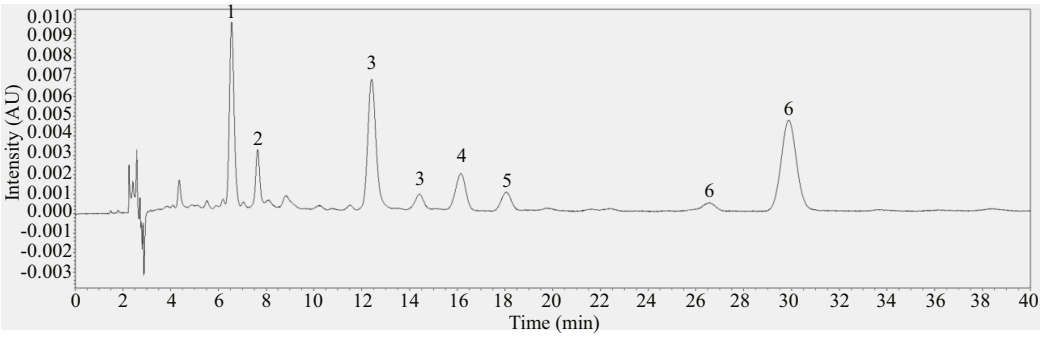

Fig.2 The chromatogram of mixed standard solution at 450 nm

Peaks assignment: 1: fucoxanthin (6.5 min); 2: β-carotene (7.5 min); 3: astaxanthin (12.5 min, 14.5 min); 4: Lutein (16.2 min); 5: zeaxanthin (18.1 min); 6: canthaxanthin (26.6 min, 29.9 min).

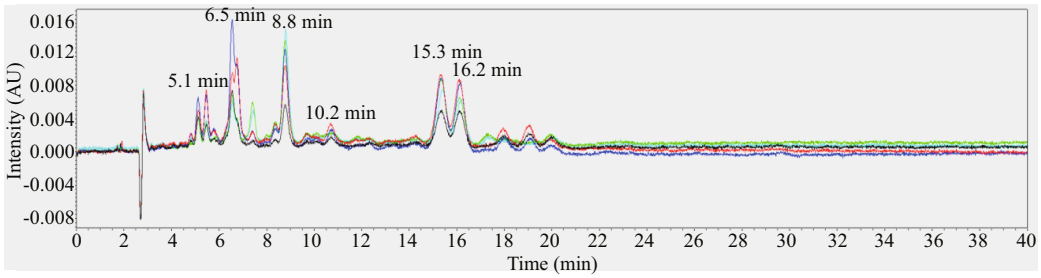

Fig.3 The chromatogram of five gray-egged female individuals at 450 nm

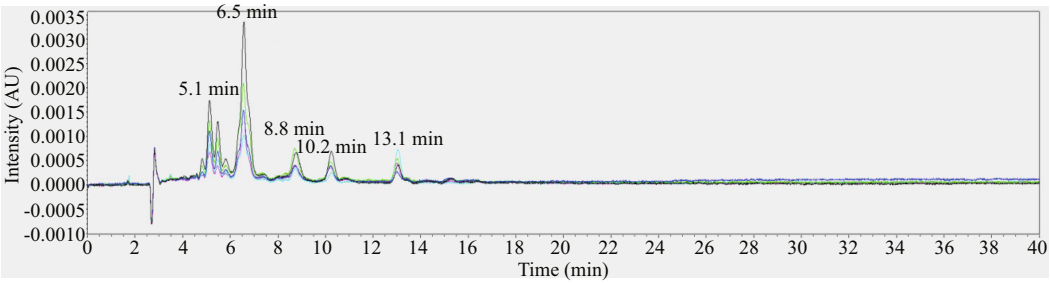

Fig.4 The chromatogram of five green-egged female individuals at 450 nm

Table 2 Comparison of the HPLC results between gray-eggs and green-eggs

Peak time (min)	5.1	6.5	8.8	10.2	13.1	15.3	16.2
Gray-egg	√	Fucoxanthin	√	√	×	√	Lutein
Green-egg	√	Fucoxanthin	√	√	√	×	×

Note: "√" means existed unknown pigment; "×" means the pigment did not exist.

shown in Fig.2. Fucoxanthin showed a peak at 6.5 min and β-carotene at 7.5 min. Astaxanthin had peaks at 12.5 min and 14.5 min. Lutein began to show a peak at 16.2 min and zeaxanthin at 18.1 min. Canthaxanthin showed peaks at 26.6 min and 29.9 min, respectively, and the characteristic peak was at 29.9 min. The six standards had obvious characteristic peaks and did not interfere with each other.

The female individuals with gray-egg mainly showed peaks at 5.1 min, 6.5 min, 8.8 min, 10.2 min, 15.3 min, and 16.2 min (Fig.3). Through comparing with the chromatogram of standards, the peak at 6.5 min can be inferred to be fucoxanthin and the peak at 16.2 min is lutein. The peaks at 5.1 min, 8.8 min, 10.2 min, and 15.3 min may be several unknown pigments. The chromatogram of female individuals with green-egg is shown in Fig.4. The peak at 6.5 min was fucoxanthin. The peaks at 5.1 min, 8.8 min and 10.2 min, consistent with the gray-egg individuals, were unknown pigments. The peak appeared at 13.1 min was the characteristic pigment. The comparison of the HPLC results between gray-eggs and green-eggs were summarized in Table 2.

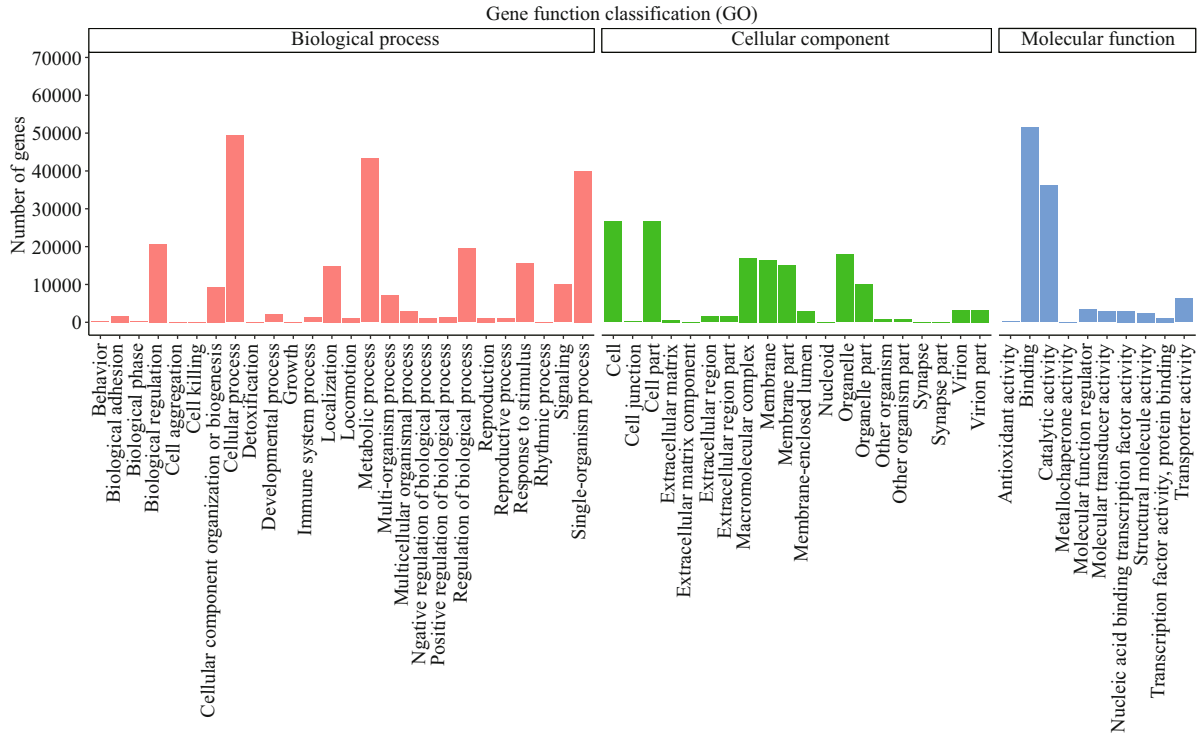

Fig.5 GO analysis of unigenes

X-axis: three GO categories including biological process (BP), cellular component (CC), and molecular function (MF); *Y*-axis: the number of unigenes assigned in the terms.

Table 3 Statistical assessment of transcriptome sequencing data

Sample	L1	L2	L3	H1	H2	H3
Raw reads	55 937 486	51 778 884	56 456 504	41 909 596	44 492 762	51 744 572
Clean reads	55 187 034	50 890 062	55 555 084	40 916 706	43 555 742	50 986 110
Q30 (%)	92.40%	92.535%	92.495%	92.13%	92.62%	92.37%
GC (%)	49.33%	49.21%	48.38%	48.57%	48.86%	48.59%
Mapped reads	29 223 396	27 176 534	30 406 468	22 928 420	24 839 594	29 895 284
Mapped ratio	52.95%	53.40%	54.73%	56.04%	57.03%	58.63%

3.2 Summary of RNA-Seq data sets

RNA-seq results are summarized in Table 3. In total, 44.56 Gb of clean data was obtained. 272 310 unigenes were assembled with a N50 of 1 524 bp and mean length of 985 bp. Q30 of each library was higher than 92%, with GC content of approximately 49%. More than 52% clean reads of each library were mapped to corresponding unigenes.

A total of 8 439 unigenes were matched successfully in all seven databases, accounting for 3.09% of the total unigenes (Table 4). A total of 89 004 (32.68%), 91 893 (33.74%), 31 200 (11.45%), and 27 357 (10.04%) unigenes were mapped to NR, GO, KOG, and KEGG databases, respectively.

Table 4 Annotation of unigenes in seven different databases

Item	Number of unigenes	Percentage (%)
NR	89 004	32.68
NT	84 228	30.93
KO	27 357	10.04
SwissProt	62 465	22.93
PFAM	91 749	33.69
GO	91 893	33.74
KOG	31 200	11.45
Annotated in all databases	8 439	3.09
Annotated in at least one database	168 411	61.84
Total unigenes	272 310	100

3.3 GO, KEGG and KOG classification

A total of 91 893 unigenes were matched to 56 GO terms and three ontologies (Fig.5). For biological process (BP), “cellular process” was the most represented term, followed by “metabolic process”

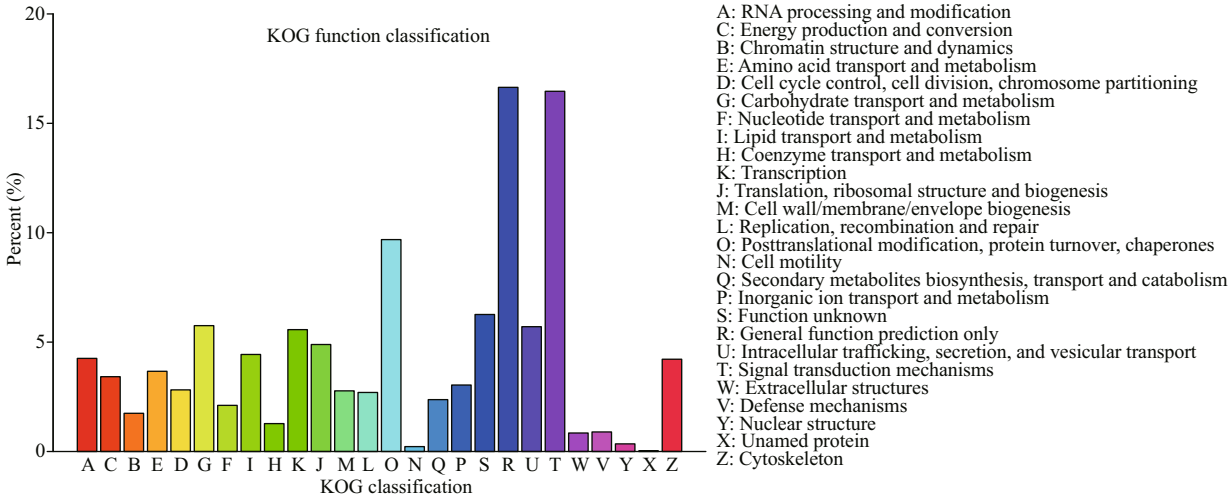

Fig.6 KOG analysis of unigenes

X-axis: the name of 26 categories in KOG; *Y*-axis: the percent of unigenes assigned in the category.

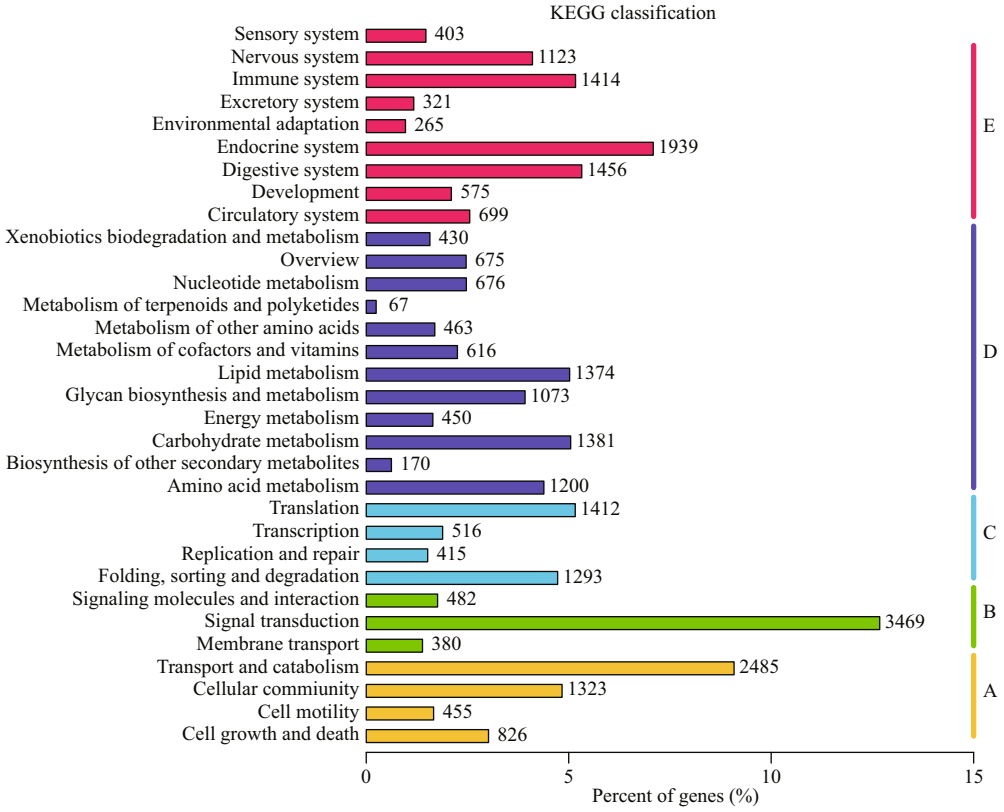

Fig.7 KEGG analysis of unigenes

X-axis: the percent of unigenes assigned in the pathway; *Y*-axis: five main branches including cellular processes (A), environmental information processing (B), genetic information processing (C), metabolism (D), and organismal systems (E).

and "single-organism process". For cellular component (CC), the highly represented terms were "cell part", "cell" and "organelle". For molecular function (MF), "catalytic activity" and "binding" were highly represented.

A total of 31 200 unigenes were successfully matched in KOG database and divided into 26 KOG categories (Fig.6). The cluster of "General function prediction only" was highly represented, followed by "Signal transduction mechanisms" and "Posttranslational modification, protein turnover, chaperones". A total of 27 357 unigenes were successfully annotated to 32 KEGG pathways in five branches (Fig.7), including cellular processes (A),

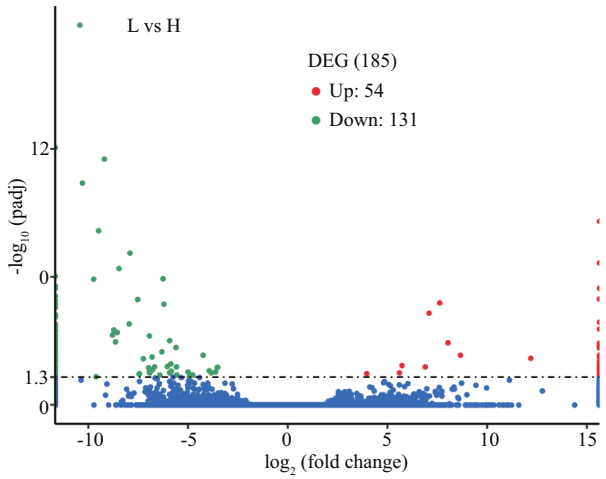

Fig.8 Volcano plot of DEGs

X-axis: the fold change of expression level of DEGs; *Y*-axis: significance of differential expression. The blue pots represent no significantly differential expression genes, while the red pots and the green pots represent up- and down-regulated genes, respectively.

environmental information processing (B), genetic information processing (C), metabolism (D) and organismal systems (E). "transport and catabolism", "signal transduction" and "endocrine system" were the most represented pathways.

3.4 Functional annotation and analysis of differentially expressed genes (DEGs)

Compared with gray-egged abalone, 185 genes were confirmed as DEGs in green samples, including 54 significantly up-regulated and 131 down-regulated genes (Fig.8). The result of hierarchical cluster analysis was shown in Fig.9. L1, L2, and L3 were clustered into a group "L", in which DEGs exhibited similar expression patterns. H1, H2, and H3 were clustered into another group "H". Compared "L" with "H", a significant difference in gene expression between green and gray egg-color can be suggested.

The top 30 of terms in GO enrichment of DEGs based on the criteria of *P*-value are listed in Fig.10, and they were classified into three functional categories (MF, BP, and CC). The numbers of GO terms in MF, BP, and CC categories were 17, 10, and 3, respectively. In MF category, the DEGs were significantly enriched in the terms of GTP binding, guanylribo nucleotide binding and guanyl nucleotide binding. In BP category, the terms significantly enriched were DNA packaging and DNA conformation change. In CC category, the DEGs were significantly enriched in extracellular region. In KEGG pathway enrichment analysis, the top 20 of pathways (*P*-value) are listed in Fig.11, including beta-alanine metabolism,

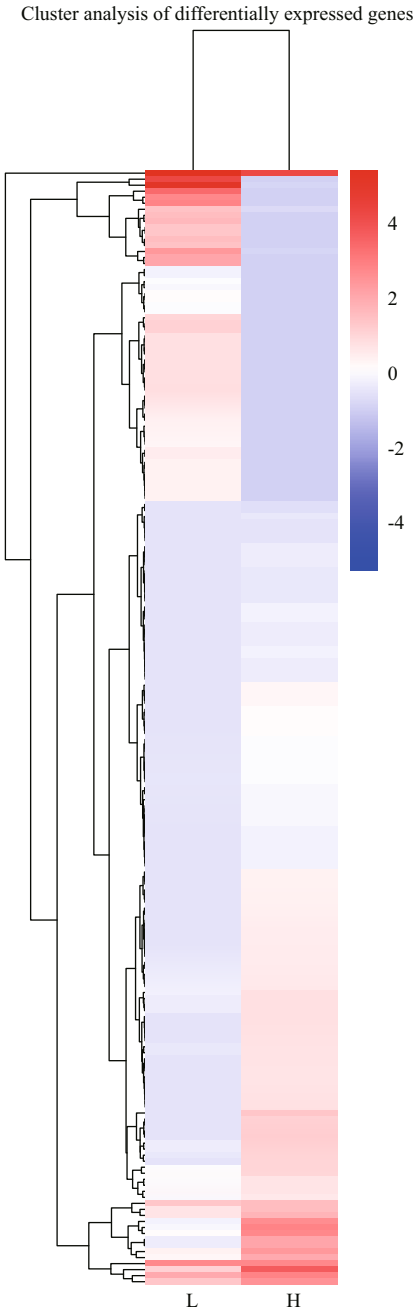

Fig.9 Hierarchical clustering analysis of DEGs between L1–3 and H1–3 samples

Different columns represent different samples, and different rows represent different genes.

nitrogen metabolism, glycerolipid metabolism, tryptophan metabolism, and so on. Of these pathways, lysosome was most abundant (6 DEGs).

3.5 Confirmation using quantitative real-time PCR

Nine genes were randomly selected for qRT-PCR analysis to confirm the reliability of DEGs data. As shown in Fig.12, the expression levels of the nine

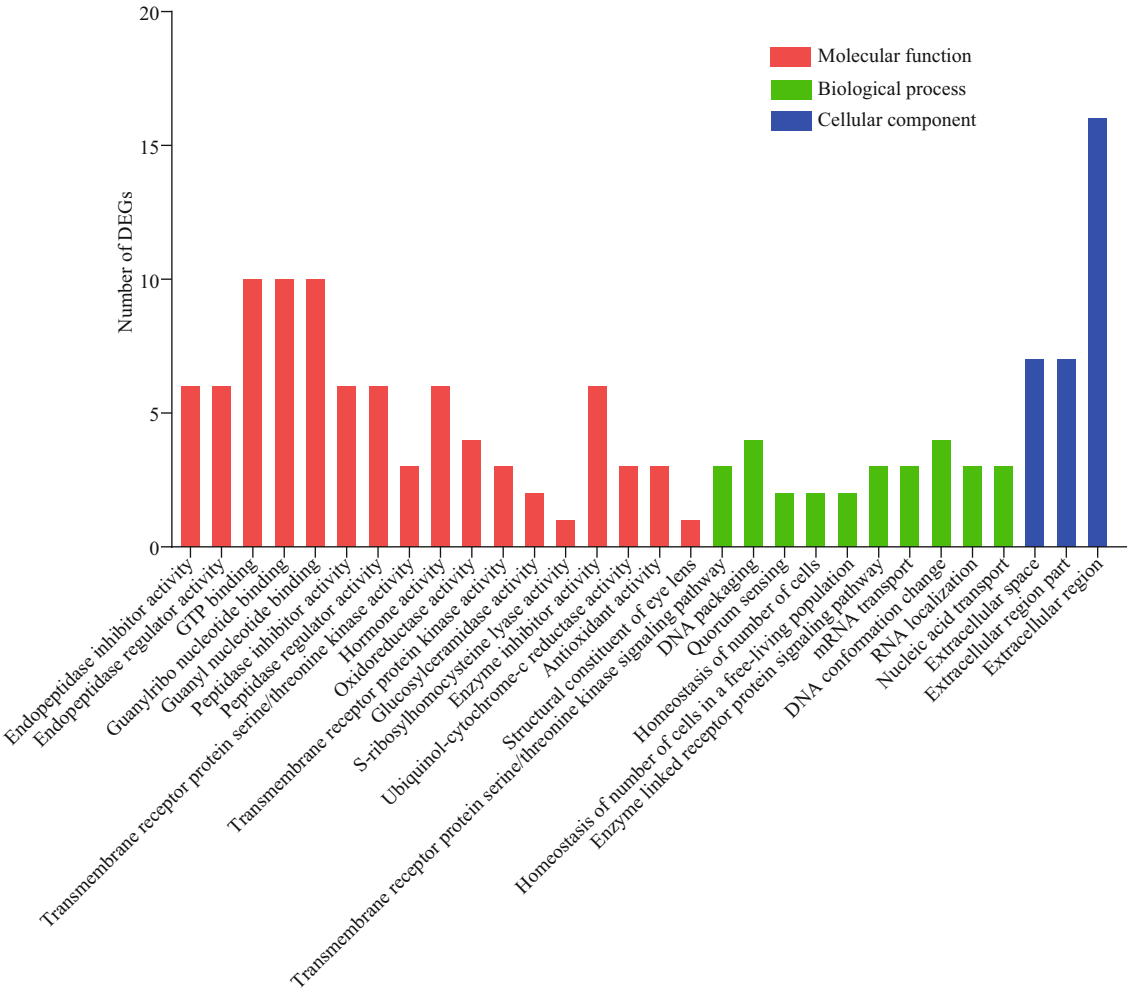

Fig.10 GO analysis of DEGs

X-axis: three GO categories including molecular function (MF), cellular component (CC) and biological process (BP); *Y*-axis: the number of DEGs.

genes analyzed by qRT-PCR are mainly in agreement with the data of RNA-seq, which indicates our RNA-seq data were reliable. The reasonable functional predictions of DEGs can be made based on enrichment analysis.

4 DISCUSSION

With the goal of exploring the genes related to the egg-color in *H. discus hannai*, the transcriptome analysis of the green- and gray-egged female individuals was firstly conducted in this study. Through analyzing transcriptome data, 185 DEGs were found. Some DEGs were involved in the terms or pathways related to the formation of egg-color in GO and KEGG analyses. The terms/pathways "flavin-containing compound metabolic process", "tyrosine metabolic process", "melanin-concentrating hormone activity", "melanosome", "pigment granule", "glutathione metabolism", "cytochrome b6f complex", "nitrogen metabolism", "alanine, aspartate and glutamate metabolism", "pigment metabolic process", and "beta-Alanine metabolism", should be paid special attention.

The pigments associated with the coloration of aquatic animals are mainly astaxanthin, lutein, β-carotene, canthaxanthin and melanin (Liu et al., 2002; Leng and Li, 2006). It has been reported that the saturation stage of animals is achieved by deepening the yellow pigment and natural lutein can be directly deposited on the scales, skin, adipose tissue, and eggs, thus showing different colors (Wang, 2012). In HPLC results, we confirmed the lutein was present in gray-egged individuals and not in green-egged individuals. In RNA-seq analysis, the term "flavin-containing compound metabolic process" was enriched and only represented by the gene "PPIP5K2". "PPIP5K2" gene was expressed in gray-egged individuals only. Therefore, the "PPIP5K2" gene was speculated on regulating the metabolism of lutein.

The terms "tyrosine metabolic process", "melanin-

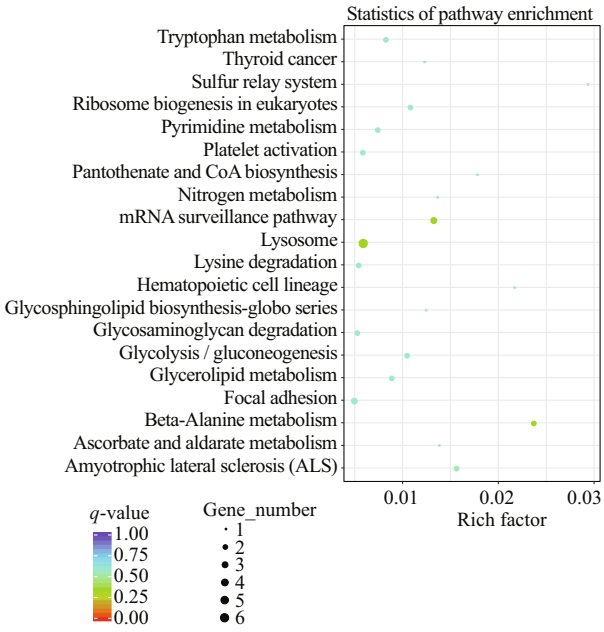

Fig.11 Scatter plot of KEGG pathways enriched by DEGs

X-axis: the rich factor of the pathways; *Y*-axis: the top 20 pathways. The size of the bubble indicates the number of DEGs enriched in the pathway, and the different colors of the bubble represent the enrichment *q*-value of the pathway. *q*-value indicates corrected *P*-value.

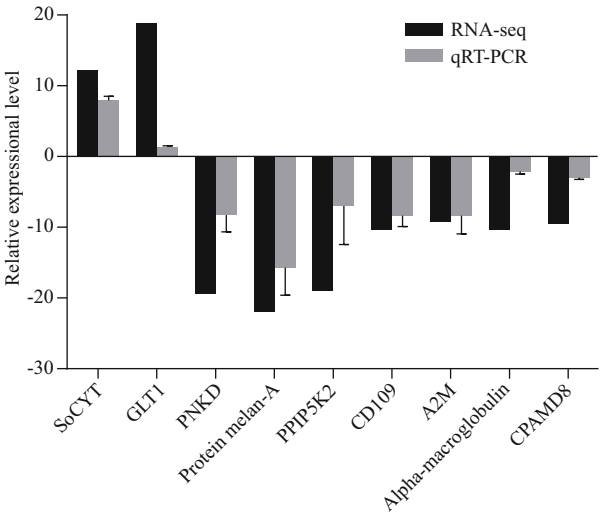

Fig.12 Validation of the selected DEGs by qRT-PCR compared with RNA-seq data

X-axis: gene name; *Y*-axis: the relative expressional level is expressed as fold-change.

concentrating hormone activity", "melanosome" and "pigment granule" were found related to the formation of egg color. It has been reported that the foot-color of *Paphia undulata* was influenced by tyrosine metabolic (Deng et al., 2018). Tyrosine is the main precursor of melanin synthesis and its metabolism process directly affects the content of melanin in cells. Melanin is considered the key pigment associated with the color formation of aquatic animals (e.g., purple and green sea cucumbers, Xing et al., (2018)). "Melanin-concentrating hormone activity", "melanosome" and "pigment granule" may play critical roles in melanin synthesis. Melanosome is a tissue-specific, lysosome-related, specialized organelle, which can synthesize and store the melanin (Raposo and Marks, 2007). Xing et al. (2017) reported that the green and purple sea cucumbers contained mature melanosomes that can secrete melanin granules into the body wall.

The pathway "Glutathione metabolism" should be significantly focused. Glutathione (c-L-glutamyl-L-cysteinyl glycine, GSH) can affect the process of pigmentation and reduce the formation of melanin by reducing the reactive oxygen species (ROS) formation and the positive modulation of GSH/GSSG ratio in cells (Pompella et al., 2003; Chu et al., 2009).

In our GO terms, "cytochrome b6f complex" was only enriched by the gene "SoCYT". "cytochrome b6f complex" is an electron transporter on the thylakoid membrane, which is composed of cytochrome b6-f complex iron-sulfur subunit protein (Staehelin and Arntzen, 1983). Its primary function is to participate in the electron transfer between photosystem I (PS I) and photosystem II (PS II), and affect the synthesis of NADPH (Zhang et al., 2001; Cassan et al., 2005). "SoCYT" gene was up-regulated in this study and its high expression was conducive to the formation of more NADPH (Liang and Li, 2016). As the coenzyme of GSH reductase, NADPH plays an important role in maintaining the content of GSH (Holmgren et al., 2005; Couto et al., 2013), which may reduce the formation of melanin. The gene "GLT1" was enriched to the "Nitrogen metabolism" and "Alanine, aspartate and glutamate metabolism" in KEGG pathway analysis. It regulates the process of glutamate metabolism with the cooperation of NADPH (Tempest et al., 1970). As the component of GSH, the synthesis of glutamate directly affects the content of GSH and then affects the formation of melanin.

In addition, "beta-alanine metabolism" was enriched in KEGG analysis. Koch et al. (2000) found that N-B-alanyldopamine synthase (BAS) transfers beta-alanine to dopamine to form N-β-alanyldopamine (NBAD), which can reduce the deposition of melanin on the body surface.

5 CONCLUSION

In this study, the pigment composition and a transcriptome analysis between green- and gray-

egged individuals of *H. discus hannai* was performed. The expression products of 185 unigenes (DEGs) exhibited significant differential expression. The DEGs involved in "flavin-containing compound metabolic process", "melanosome", "glutathione metabolism" and "cytochrome b6f complex" were identified and found to be related to the formation of egg-color, which merits further investigation. Our results provide foundational information for the functional analysis of egg-color related genes and are beneficial to the selective breeding of *H. discus hannai*.

6 DATA AVAILABILITY STATEMENT

All data that support the findings of this study are available from the corresponding author on reasonable request.

References

Altschul S F, Gish W, Miller W, Myers E W, Lipman D J. 1990. Basic local alignment search tool. *Journal of Molecular Biology*, **215**(3): 403-410, https://doi.org/10.1016/S0022-2836(05)80360-2.

Apweiler R, Bairoch A, Wu C H, Barker W C, Boeckmann B, Ferro S, Gasteiger E, Huang H Z, Lopez R, Magrane M, Martin M J, Natale D A, O'Donovan C, Redaschi N, Yeh L S L. 2004. UniProt: the Universal Protein knowledgebase. *Nucleic Acids Research*, **32**(S1): D115-D119, https://doi.org/10.1093/nar/gkh131.

Ashburner M, Ball C A, Blake J A, Botstein D, Butler H, Cherry J M, Davis A P, Dolinski K, Dwight S S, Eppig J T, Harris M A, Hill D P, Issel-Tarver L, Kasarskis A, Lewis S, Matese J C, Richardson J E, Ringwald M, Rubin G M, Sherlock G. 2000. Gene ontology: tool for the unification of biology. *Nature Genetics*, **25**(1): 25-29, https://doi.org/10.1038/75556.

Cassan N, Lagoutte B, Sétif P. 2005. Ferredoxin-$NADP^+$ Reductase kinetics of electron transfer, transient intermediates, and catalytic activities studied by flash-absorption spectroscopy with isolated photosystem I and ferredoxin. *Journal of Biological Chemistry*, **280**(28): 25 960-25 972, https://doi.org/10.1074/jbc.M503742200.

Choi M J, Kim G D, Kim J M, Lim H K. 2015. Differentially-expressed genes associated with faster growth of the Pacific abalone, *Haliotis discus hannai*. *International Journal of Molecular Sciences*, **16**(11): 27 520-27 534, https://doi.org/10.3390/ijms161126042.

Chu H L, Wang B S, Duh P D. 2009. Effects of selected organo-sulfur compounds on melanin formation. *Journal of Agricultural and Food Chemistry*, **57**(15): 7 072-7 077, https://doi.org/10.1021/jf9005824.

Cooley J M. 1971. The effect of temperature on the development of resting eggs of *Diaptomus oregonensis* Lillj (Copepoda: Calanoida). *Limnology and Oceanography*, **16**(6): 921-926, https://doi.org/10.4319/lo.1971.16.6.0921.

Couto N, Malys N, Gaskell S J, Barber J. 2013. Partition and turnover of glutathione reductase from *Saccharomyces cerevisiae*: a proteomic approach. *Journal of Proteome Research*, **12**(6): 2 885-2 894, https://doi.org/10.1021/pr4001948.

Deng S Z, Zhang X L, Li Q C, Zhang J, Han F, Liu X D. 2018. Comparative transcriptome analysis of *Paphia undulata* with different foot colors. *Marine Genomics*, **42**: 25-31, https://doi.org/10.1016/j.margen.2018.08.007.

Deng Y Y, Li J Q, Wu S F, Zhu Y P, Chen Y W, He F C. 2006. Integrated nr database in protein annotation system and its localization. *Computer Engineering*, **32**(5): 71-73, 76. (in Chinese with English abstract)

Ding J, Zhao L, Chang Y Q, Zhao W M, Du Z L, Hao Z L. 2015. Transcriptome sequencing and characterization of Japanese scallop *Patinopecten yessoensis* from different shell color lines. *PLoS One*, **10**(2): e0116406, https://doi.org/10.1371/journal.pone.0116406.

Finn R D, Bateman A, Clements J, Coggill P, Eberhardt R Y, Eddy S R, Heger A, Hetherington K, Holm L, Mistry J, Sonnhammer E L L, Tate J, Punta M. 2013. Pfam: the protein families database. *Nucleic Acids Research*, **42**(D1): D222-D230, https://doi.org/10.1093/nar/gkt1223.

Gordon H R, Cook P A. 2004. World abalone fisheries and aquaculture update: supply and market dynamics. *Journal of Shellfish Research*, **23**(4): 935-939.

Guo H, Ye C X, Wang A L, Xian J A, Liao S A, Miao Y T, Zhang S P. 2013. Trascriptome analysis of the Pacific white shrimp *Litopenaeus vannamei* exposed to nitrite by RNA-seq. *Fish & Shellfish Immunology*, **35**(6): 2 008-2 016, https://doi.org/10.1016/j.fsi.2013.09.019.

Harney E, Dubief B, Boudry P, Basuyaux O, Schilhabel M B, Huchette S, Paillard C, Nunes F L D. 2016. *De novo* assembly and annotation of the European abalone *Haliotis tuberculata* transcriptome. *Marine Genomics*, **28**: 11-16, https://doi.org/10.1016/j.margen.2016.03.002.

Holmgren A, Johansson C, Berndt C, Lönn M E, Hudemann C, Lillig C H. 2005. Thiol redox control via thioredoxin and glutaredoxin systems. *Biochemical Society Transactions*, **33**(6): 1 375-1 377, https://doi.org/10.1042/BST0331375.

Huerta-Cepas J, Szklarczyk D, Forslund K, Cook H, Heller D, Walter M C, Rattei T, Mende D R, Sunagawa S, Kuhn M, Jensen L J, von Mering C, Bork P. 2015. eggNOG 4.5: a hierarchical orthology framework with improved functional annotations for eukaryotic, prokaryotic and viral sequences. *Nucleic Acids Research*, **44**(D1): D286-D293, https://doi.org/10.1093/nar/gkv1248.

Hulet R M, Marquez B J, Molle E, Flegal C J. 1978. Relationship of pheasant egg color and hatchability. *Poultry Science*, **57**(4): 1 146-1 148.

Jeukens J, Renaut S, ST-CYR J, Nolte A W, Bernatchez L. 2010. The transcriptomics of sympatric dwarf and normal lake whitefish (*Coregonus clupeaformis* spp., *Salmonidae*) divergence as revealed by next-generation sequencing. *Molecular Ecology*, **19**(24): 5 389-5 403, https://doi.org/10.1111/j.1365-294X.2010.04934.x.

Kanehisa M, Goto S, Kawashima S, Okuno Y, Hattori M. 2004. The KEGG resource for deciphering the genome. *Nucleic Acids Research*, **32**(S1): D277-D280, https://doi.org/10.1093/nar/gkh063.

Kim M A, Rhee J S, Kim T H, Lee J S, Choi A Y, Choi B S, Choi I Y, Sohn Y C. 2017. Alternative splicing profile and sex-preferential gene expression in the female and male Pacific Abalone *Haliotis discus hannai*. *Genes*, **8**(3): 99, https://doi.org/10.3390/genes8030099.

Koch P B, Behnecke B, Weigmann-Lenz M, Ffrench-Constant R H. 2000. Insect pigmentation: activities of β-alanyldopamine synthase in wing color patterns of wild-type and melanic mutant swallowtail butterfly *Papilio glaucus*. *Pigment Cell Research*, **13**(S8): 54-58, https://doi.org/10.1111/j.0893-5785.2000.130811.x.

Leng X J, Li X Q. 2006. The recent advance of aquatic animal pigmentation. *Journal of Fisheries of China*, **30**(1): 138-143. (in Chinese with English abstract)

Li B, Dewey C N. 2011. RSEM: accurate transcript quantification from RNA-Seq data with or without a reference genome. *BMC Bioinformatics*, **12**(1): 323.

Li H, Durbin R. 2009. Fast and accurate short read alignment with Burrows-Wheeler transform. *Bioinformatics*, **25**(14): 1 754-1 760, https://doi.org/10.1093/bioinformatics/btp324.

Liang P X, Li Y R. 2016. Cloning of cytochrome b6-f complex iron-sulfur subunit (SoCYT) from sugarcane and analysis of its expression under PEG stress. *Southwest China Journal of Agricultural Sciences*, **29**(5): 1 032-1 037, https://doi.org/10.16213/j.cnki.scjas.2016.05.008. (in Chinese with English abstract)

Liu J H, Wang A L, Wang W N, Liu F S. 2002. Progress of study on the component of pigment and painting substance of aquatic animals. *Chinese Journal of Zoology*, **37**(3): 92-96, https://doi.org/10.13859/j.cjz.2002.03.024. (in Chinese with English abstract)

Liu Z Q, Lin S, Baker P J, Wu L F, Wang X R, Wu H, Xu F, Wang H Y, Brathwaite M E, Zheng Y G. 2015. Transcriptome sequencing and analysis of the entomopathogenic fungus *Hirsutella sinensi*s isolated from *Ophiocordyceps sinensis*. *BMC Genomics*, **16**(1): 106, https://doi.org/10.1186/s12864-015-1269-y.

Livak K J, Schmittgen T D. 2001. Analysis of relative gene expression data using real-time quantitative PCR and the $2^{-\Delta\Delta Ct}$ method. *Methods*, **25**(4): 402-408, https://doi.org/10.1006/meth.2001.1262.

Mao X Z, Cai T, Olyarchuk J G, Wei L P. 2005. Automated genome annotation and pathway identification using the KEGG Orthology (KO) as a controlled vocabulary. *Bioinformatics*, **21**(19): 3 787-3 793, https://doi.org/10.1093/bioinformatics/bti430.

Metzker M L. 2010. Sequencing technologies-the next generation. *Nature Reviews Genetics*, **11**(1): 31-46, https://doi.org/10.1038/nrg2626.

Nam B H, Jung M, Subramaniyam S, Yoo S I, Markkandan K, Moon J Y, Kim Y O, Kim D G, An C M, Shin Y, Jung H J, Park J H. 2016. Transcriptome analysis revealed changes of multiple genes involved in *Haliotis discus hannai* innate immunity during *Vibrio parahemolyticus* infection. *PLoS One*, **11**(4): e0153474, https://doi.org/10.1371/journal.pone.0153474.

Pompella A, Visvikis A, Paolicchi A, De Tata V, Casini A F. 2003. The changing faces of glutathione, a cellular protagonist. *Biochemical Pharmacology*, **66**(8): 1 499-1 503, https://doi.org/10.1016/S0006-2952(03)00504-5.

Raposo G, Marks M S. 2007. Melanosomes—dark organelles enlighten endosomal membrane transport. *Nature Reviews Molecular Cell Biology*, **8**(10): 786-797, https://doi.org/10.1038/nrm2258.

Shen Y W, Huang Z K, Liu G M, Ke C H, You W W. 2019. Hemolymph and transcriptome analysis to understand innate immune responses to hypoxia in Pacific abalone. *Comparative Biochemistry and Physiology Part D*: *Genomics and Proteomics*, **30**: 102-112, https://doi.org/10.1016/j.cbd.2019.02.001.

Staehelin L A, Arntzen C J. 1983. Regulation of chloroplast membrane function: protein phosphorylation changes the spatial organization of membrane components. *The Journal of Cell Biology*, **97**(5): 1 327-1 337, https://doi.org/10.1083/jcb.97.5.1327.

Symonds J E, Moss G, Jopson N B, Roberts R, Birss J, Heath P, Walkera S P, Andersonf R M, McEwan K M, Amer P R. 2012. Family-based selective breeding of New Zealand abalone, *Haliotis iris*: challenges and opportunities. *Proceedings of the New Zealand Society of Animal Production*, **72**: 216-221.

Tempest D W, Meers J L, Brown C M. 1970. Synthesis of glutamate in *Aerobacter aerogenes* by a hitherto unknown route. *Biochemical Journal*, **117**(2): 405-407, https://doi.org/10.1042/bj1170405.

Trapnell C, Williams B A, Pertea G, Mortazavi A, Kwan G, Van Baren M J, Salzberg S L, Wold B J, Pachter L. 2010. Transcript assembly and quantification by RNA-Seq reveals unannotated transcripts and isoform switching during cell differentiation. *Nature Biotechnology*, **28**(5): 511-515, https://doi.org/10.1038/nbt.1621.

Valenzuela-Miranda D, Del Río-Portilla M A, Gallardo-Escárate C. 2015. Characterization of the growth-related transcriptome in California red abalone (*Haliotis rufescens*) through RNA-Seq analysis. *Marine Genomics*, **24**: 199-202, https://doi.org/10.1016/j.margen.2015.05.009.

Wang C H, Wachholtz M, Wang J, Liao X L, Lu G Q. 2014. Analysis of the skin transcriptome in two Oujiang color varieties of common carp. *PLoS One*, **9**(3): e90074, https://doi.org/10.1371/journal.pone.0090074.

Wang L B. 2012. Effect of natural xanthophylls on growth performance, skin coloring and antioxidant function in yellow catfish (*Pelteobagrus fulvidraco*) and its metabolic regulation in fish tissues. Chinese Academy of Agricultural Sciences, Beijing. (in Chinese with English abstract)

Wang S. 2015. Study on the selection of reference genes and the expression regulation of C-type lectin gene in *Haliotis discus hannai*. Shanghai Ocean University, Shanghai. (in Chinese with English abstract)

Xing L L, Sun L N, Liu S L, Li X N, Miao T, Zhang L B, Yang

H S. 2017. Comparison of pigment composition and melanin content among white, light-green, dark-green, and purple morphs of sea cucumber, *Apostichopus japonicus*. *Acta Oceanologica Sinica*, **36**(12): 45-51, https://doi.org/10.1007/s13131-017-1056-5.

Xing L L, Sun L N, Liu S L, Li X N, Zhang L B, Yang H S. 2018. De Novo assembly and comparative transcriptome analyses of purple and green morphs of *Apostichopus japonicus* during body wall pigmentation process. *Comparative Biochemistry and Physiology Part D*: *Genomics and Proteomics*, **28**: 151-161, https://doi.org/10.1016/j.cbd.2018.09.001.

You W W, Ke C H, Luo X, Wang D X, 2009. Growth and survival of three small abalone *Haliotis diversicolor* populations and their reciprocal crosses. *Aquaculture Research*, **40**(13): 1 474-1 480, https://doi.org/10.1111/j.1365-2109.2009.02247.x.

Young M D, Wakefield M J, Smyth G K, Oshlack A. 2010. Gene ontology analysis for RNA-seq: accounting for selection bias. *Genome Biology*, **11**(2): R14, https://doi.org/10.1186/gb-2010-11-2-r14.

Zhang H, Whitelegge J P, Cramer W A. 2001. Ferredoxin: $NADP^+$ oxidoreductase is a subunit of the chloroplast cytochrome b_6f complex. *Journal of Biological Chemistry*, **276**(41): 38 159-38 165, https://doi.org/10.1074/jbc.M105454200.

Zhang X, Shi J L, Sun Y L, Habib Y J, Yang H P, Zhang Z P, Wang Y L. 2019. Integrative transcriptome analysis and discovery of genes involving in immune response of hypoxia/thermal challenges in the small abalone *Haliotis diversicolor*. *Fish & Shellfish Immunology*, **84**: 609-626, https://doi.org/10.1016/j.fsi.2018.10.044.

Zhao H F, Feng Y W, Liu X Q, Jiang X, Wei X M, Liu J L, Jiang H L. 2016. Growth and immune diversity of *Haliotis discus hannai* juvenile abalone with different egg colors. *Progress in Fishery Sciences*, **37**(6): 110-114, https://doi.org/10.11758/yykxjz.20150810001. (in Chinese with English abstract)